

# R-Modes in the ocean of a magnetic neutron star

V. Rezanian

*Theoretical Physics Institute, Department of Physics, University of Alberta  
Edmonton, AB, Canada, T6G 2J1*

*Institute for Advanced Studies in Basic Sciences, Zanjan 45195, Iran*

## ABSTRACT

We study the dynamics of r-modes in the ocean of a magnetic neutron star. We modeled the star's ocean with a spherical rotating thin shell and assumed that the magnetic field symmetry axis is not aligned to the shell's spin axis. In the magnetohydrodynamic approximation, we calculate the frequency of  $\ell = m$  r-modes in the shell of an incompressible fluid. Different r-modes with  $\ell$  and  $\ell \pm 2$  are coupled by the *inclined* magnetic field. Kinematical secular effects for the motion of a fluid element in the shell undergoing  $\ell = m = 2$  r-mode are studied. The magnetic corrected drift velocity of a given fluid element undergoing the  $\ell = m$  r-mode oscillations is obtained. The magnetic field increases the magnitude of the fluid drift produced by the r-mode oscillations. The drift velocity is strongly modulated by the inclined magnetic field. We show that the magnetic field is distorted by the high- $\ell$  magnetic r-modes more strongly than by the low- $\ell$  modes. Further, due to the shear produced by the r-mode drift velocity, the high- $\ell$  modes in the ocean fluid will damp faster than the low- $\ell$  ones.

*Subject headings:* stars: neutron – stars: magnetic – stars: rotation – stars: oscillations

## 1. Introduction

In a series of papers Bildsten et al. (1995, 1996) showed that neutron stars accreting at high accretion rates  $\gtrsim 10^{-9} \text{ M}_{\odot} \text{ yr}^{-1}$  are covered with massive oceans with densities  $\gtrsim 10^9 \text{ g cm}^{-3}$ . Both theoretical consideration of the nature of burning at these rates (Fushiki & Lamb 1987; Bildsten 1993, 1995) and observational features of type I X-ray bursts (van der Klis

1995) reveal that the star burns the accreting hydrogen and helium to mid-weight elements like C, O, Ne, etc., and accumulates a massive ( $\sim 10^{-6} M_{\odot}$ ) degenerate liquid ocean. Fusion of this fuel to iron-group elements does not occur until densities  $\gtrsim 10^9 \text{ g cm}^{-3}$ . The neutron stars with lower accreting rates (the atoll sources) burn the accreted hydrogen and helium directly to iron-group elements via the type I X-ray bursts which are crystallized by the larger Coulomb force at much lower densities. Further, they conjectured that the waves in these oceans might modulate the outgoing X-ray flux at frequencies comparable to what is observed.

In this paper, motivated by Bildsten et al. conjecture we study the evolution of r-modes in the ocean of magnetic neutron stars. The r-modes those are analogous to the Rossby waves in the earth’s oceans, are driven by the Coriolis force in the rotating stars. Their motions are dominantly toroidal and their oscillation frequencies are proportional to the rotation rate of the star,  $\Omega$ . Since even the small magnitude of Coriolis force drives r-modes in a rotating fluid, they should be considered in the dynamics of the fluid. We model the star’s ocean with a thin rotating shell of incompressible inviscid fluid at the radius  $R$  which is sandwiched between two hard spheres. The role of spheres is to make sure that the fluid motion is restricted to a two-dimensional spherical surface, so, there is no friction between spheres and the fluid.

The paper is organized as follow. In the next section, we set up the magnetohydrodynamics equations for a spherical thin shell in the background of a uniform magnetic field in which magnetic field symmetry axis is not aligned with shell’s spin axis. We find the magnetic coupling coefficients and then the corrected eigenfrequencies and eigenvectors for  $\ell = m$  r-mode. In section 3 we consider the kinematical secular drift of r-modes, introduced by Rezzolla et al. (2000, 2001a,b), in a magnetic ocean fluid. We show that as well as the magnetic field strength causes the drift magnitude to increase, the inclination of the magnetic field axis modulates the r-mode trajectories. The latter did not consider in the previous studies. Section 4 is devoted for further discussions.

## 2. R-modes in magnetic rotating shell

Historically, the study of oscillations of fluids in a rotating shell in the presence of a magnetic field has been started about fifty years ago by geophysicists. Pioneering works by Hide (1966) and Stewartson (1966), are concerned with Earth’s core magnetic modes

that may be accounted to the observed secular changes in the main geomagnetic field at the Earth’s surface. It is well known that the Earth’s magnetic field at the surface drifts westward slowly, with the period of the order of one thousand years. They assumed an unrealistic magnetic field configuration characterized by a toroidal field of constant magnitude on the shell, and found the magnetic corrected toroidal motions might cause the field drift at the surface of the Earth.

In this paper we investigate the MHD perturbations of a uniformly rotating thin spherical shell of incompressible fluid of radius  $R$ , endowed with a uniform magnetic field (more realistic configuration) which is given by

$$\mathbf{B} = B_p (\cos \theta \mathbf{e}_{\hat{r}} - \sin \theta \mathbf{e}_{\hat{\theta}}), \quad (1)$$

on the shell. Since the shell is sandwiched between two spherical hard covers, the motion of the fluid is restricted to a two-dimensional spherical surface. Further, we assume the symmetry axis of the field makes an angle  $\beta$  to the shell’s rotation axis. We work in an ideal MHD framework, so that the field lines are frozen into the fluid, and the magnetic field rotates at the same rate as the shell.

For an uniformly rotating shell of incompressible fluid with angular frequency  $\Omega$  around the  $z$ -axis, the fluid velocity perturbation field in the corotating frame is exactly determined by

$$\delta \mathbf{v} = \alpha \dot{\boldsymbol{\xi}}_{\ell m}, \quad (2a)$$

$$\boldsymbol{\xi}_{\ell m}(\theta, \phi, t) = \frac{U_{\ell m}(R)}{R} \left( -\partial_{\phi} Y_{\ell m}(\theta, \phi) / \sin \theta \mathbf{e}_{\hat{\theta}} + \partial_{\theta} Y_{\ell m}(\theta, \phi) \mathbf{e}_{\hat{\phi}} \right) e^{-i\omega_{\ell m} t}, \quad (2b)$$

for any arbitrary function  $U_{\ell m}(R)$  and with dispersion relation

$$\omega_{\ell m} = -\frac{2m\Omega}{\ell(\ell+1)}. \quad (2c)$$

Here  $\alpha$  is the amplitude of the mode. Equation (2) is the exact solution of the fluid equations of motion in fully nonlinear regime, see Levin & Ushomirsky (2001) for more detail and references therein.

Recently, Morsink & Rezanian (2002) (MR) have studied dynamics of a rotating star in the presence of a magnetic field in which its symmetric axis is not aligned to the star’s spin axis. For the  $\ell = m$  r-modes of an incompressible rotating fluid in the background of uniform magnetic field they obtained a shift proportional to the ratio of the magnetic energy to the rotational energy of the star in the r-mode eigenfrequencies, only.

Following MR, we consider the magnetic force, produced by the fluid's perturbations of the rotating shell, drives the motion of fluid elements. As they've shown, the eigenvalue equation for eigenfrequencies and eigenvectors of the normal modes of fluid in the presence of magnetic field will be corrected by

$$\omega_A \left( c_A - \frac{\mathcal{M}}{2\epsilon_A} \sum_D \kappa_{AD} c_D \right) = \sigma_A c_A, \quad (3)$$

where the  $c_A$  and  $\sigma_A$  are the magnetic corrected eigenvector and eigenfrequency in the rotating frame, respectively. Here  $\epsilon_A$  is the energy of the mode in the rotating frame. The magnetic coupling coefficients,  $\kappa_{AD}$ , can be calculated on the surface of sphere as

$$\kappa_{AD} = -\frac{1}{4\pi\mathcal{M}} \int \delta\mathbf{B}_A^* \cdot \delta\mathbf{B}_D d\Omega, \quad (4)$$

$$\delta\mathbf{B}_A = \nabla \times (\boldsymbol{\xi}_A \times \mathbf{B}), \quad (4a)$$

where  $\mathcal{M} = B_p^2/4\pi$  is the magnetic field energy density<sup>1</sup>. Note that in the above calculations we expand any perturbation vectors in terms of the modes of rotating star,  $\boldsymbol{\xi}_A$ , as

$$\boldsymbol{\xi} = \sum_A c_A \boldsymbol{\xi}_A e^{-i\sigma t}. \quad (5)$$

Here upper-case Latin subscripts are used to label solutions and corresponds to the unique set of quantum numbers which describe the solutions.

To calculate the magnetic coupling we use the method that is described by MR. They used the spin-weighted formalism in which: (a) the vectors are expressed in the orthonormal but complex basis  $\{\mathbf{e}_+, \mathbf{e}_-\}$  that is related to the usual orthonormal basis  $\{\mathbf{e}_\theta, \mathbf{e}_\phi\}$  by

$$\mathbf{e}_\pm = \frac{1}{\sqrt{2}} (\mathbf{e}_\theta \pm \mathbf{e}_\phi); \quad (6)$$

(b) all functions are expanded by spin-weighted spherical harmonics,  ${}_sY_{\ell m}(\theta, \phi)$ , that are defined by (Campbell 1971)

$${}_sY_{\ell m}(\theta, \phi) = \sqrt{\frac{(2\ell+1)}{4\pi}} d_{-sm}^\ell(\theta) e^{im\phi} \quad (7)$$

---

<sup>1</sup>Equation (1) leads  $\nabla \times \mathbf{B} = 0$ . As a result, the term containing  $\mathbf{J}$  vanishes. The term containing  $\boldsymbol{\xi} \times \mathbf{B}$  does not vanish, but its contribution is smaller by  $\Omega^2 R^2/c^2$  for r-modes and we neglect it in equation 4.

where the  $d_{sm}^\ell(\theta)$  are the matrix representations for rotations through an angle  $\theta$  discussed in detail by Edmonds (1974). When  $s = 0$ , the spin-weighted spherical harmonics reduce to the regular spherical harmonics. The orthogonality relations are

$$\int_{4\pi} {}_sY_{\ell'm'}^* {}_sY_{\ell m} d\Omega = \delta_{\ell\ell'} \delta_{mm'}. \quad (8)$$

We use the convention that  ${}_sY_{\lambda\mu}^*(\theta, \phi) = (-1)^{\sigma+\mu} {}_{-s}Y_{\lambda-\mu}(\theta, \phi)$ .

A uniform magnetic field tilted by an angle  $\beta$  from the shell's spin axis can be written in spin-weight formalism as

$$\mathbf{B}(\theta, \phi) = \sum_{\bar{m}=-1}^{\bar{m}=1} \left( b_0^{1,\bar{m}}(a) {}_0Y_{1\bar{m}}(\theta, \phi) \mathbf{e}_0 + b_+^{1,\bar{m}}(a) {}_{+1}Y_{1\bar{m}}(\theta, \phi) \mathbf{e}_- + b_-^{1,\bar{m}}(a) {}_{-1}Y_{1\bar{m}}(\theta, \phi) \mathbf{e}_+ \right) \quad (9)$$

where the functions  $b_s^{1,\bar{m}}(a)$  are given by

$$b_{\pm}^{1,\bar{m}} = \mp b_0^{1,\bar{m}} = \sqrt{\frac{4\pi}{3}} d_{\bar{m}0}^1(\beta), \quad (10)$$

and the  $d_{\bar{m}0}^1$  are given by

$$d_{10}^1(\beta) = \frac{1}{\sqrt{2}} \sin \beta, \quad d_{00}^1(\beta) = \cos \beta, \quad d_{-10}^1(\beta) = -\frac{1}{\sqrt{2}} \sin \beta. \quad (11)$$

To rewrite equation (2) in spin-weighted formalism, at first we normalize  $\boldsymbol{\xi}$  such that the energy density of the modes in the corotating system is  $\epsilon_A = \mathcal{T}$ , where  $\mathcal{T}$  is rotational kinetic energy density of the shell. Therefore the r-modes of non-magnetic incompressible thin shell have the form

$$\omega_{\ell_A m_A} = -\frac{2m_A \Omega}{\ell_A(\ell_A + 1)} \quad (12a)$$

$$U_{\ell_A m_A} = R^2 \sqrt{\frac{\ell_A(\ell_A + 1)}{4m_A^2}} \quad (12b)$$

$$\epsilon_{\ell_A m_A} = \mathcal{T} = \frac{1}{2} \rho R^2 \Omega^2, \quad (12c)$$

The spin-weighted decomposition of the  $A$ th r-mode is

$$\xi_A(x) = f_+^A {}_{+1}Y_{\ell_A m_A} \mathbf{e}_- + f_-^A {}_{-1}Y_{\ell_A m_A} \mathbf{e}_+, \quad (13)$$

where the functions  $f_s^A(r)$  are given by (Schenk et al. (2001))

$$f_+^A = f_-^A = \frac{R}{2\sqrt{2}} \frac{\ell(\ell_A + 1)}{m_A}. \quad (14)$$

Different components of the perturbed magnetic field,  $\delta \mathbf{B}_A$ , due to the r-modes in the thin shell, can be found in spin-weighted formalism as

$$\delta B_{A,s}(\theta, \phi) = \sum_{\lambda, \mu} \delta B_{A,s}^{\lambda, \mu} Y_{\lambda \mu}^*, \quad (15)$$

$$\begin{aligned} \delta B_{A,0}^{\lambda, \mu} &= \sum_{\bar{m}=-1}^{+1} C(\ell_A, 1, \lambda) \begin{pmatrix} \lambda & \ell_A & 1 \\ \mu & m_A & \bar{m} \end{pmatrix} \begin{pmatrix} \lambda & \ell_A & 1 \\ 0 & -1 & 1 \end{pmatrix} \frac{1}{a} b_0^{1, \bar{m}} f_+^A (1 + (-1)^{\lambda + \ell_A}) \\ \delta B_{A,+}^{\lambda, \mu} &= (-1)^{\lambda + \ell_A + 1} \delta B_{A,-}^{\lambda, \mu} \end{aligned} \quad (15b)$$

$$\begin{aligned} &= - \sum_{\bar{m}=-1}^{+1} C(\ell_A, 1, \lambda) \begin{pmatrix} \lambda & \ell_A & 1 \\ \mu & m_A & \bar{m} \end{pmatrix} \frac{1}{a} b_0^{1, \bar{m}} f_+^A \times \\ &\quad \left[ \sqrt{\frac{\ell_A(\ell_A + 1)}{2}} \begin{pmatrix} \lambda & \ell_A & 1 \\ -1 & 0 & 1 \end{pmatrix} + \sqrt{\frac{(\ell_A - 1)(\ell_A + 2)}{2}} \begin{pmatrix} \lambda & \ell_A & 1 \\ -1 & 2 & -1 \end{pmatrix} \right], \end{aligned} \quad (15c)$$

where  $\begin{pmatrix} \ell & k & \lambda \\ -s & -t & -\sigma \end{pmatrix}$  is a Wigner 3-j symbol (Edmonds 1974) and the constant  $C(\ell_A, \bar{\ell}, \lambda)$  is defined by

$$C(\ell_A, \bar{\ell}, \lambda) = (-1)^{\ell_A + \lambda + \bar{\ell}} \sqrt{\frac{(2\ell_A + 1)(2\bar{\ell} + 1)(2\lambda + 1)}{4\pi}}. \quad (16)$$

In equation (15)  $\lambda$  takes on values  $\ell_A, \ell_A \pm 1$ , although Eq. (15a) will survive only for  $\lambda = \ell_A$ . Since the spin-weighted spherical harmonics obey the orthogonality relation (8), integrals over all angles of quantities quadratic in  $\delta \mathbf{B}$  have the simple form

$$\kappa_{AD} = \int \delta \mathbf{B}_A^* \cdot \delta \mathbf{B}_D d\Omega = \sum_{\lambda, \mu} \left( \delta B_{A,0}^{*\lambda, \mu} \delta B_{D,0}^{\lambda, \mu} + \delta B_{A,+}^{*\lambda, \mu} \delta B_{D,+}^{\lambda, \mu} + \delta B_{A,-}^{*\lambda, \mu} \delta B_{D,-}^{\lambda, \mu} \right), \quad (17)$$

$$= \sum_{\lambda, \mu} \left[ \delta B_{A,0}^{*\lambda, \mu} \delta B_{D,0}^{\lambda, \mu} \delta_{AD} + \delta B_{A,+}^{*\lambda, \mu} \delta B_{D,+}^{\lambda, \mu} (1 + (-1)^{\ell_A + \ell_D}) \right], \quad (17a)$$

where  $\delta_{AD}$  is the Kronecker delta function. The last step is due to the symmetry property (15b). It then follows that the magnetic coupling coefficients between r-modes is zero unless both modes have the same parity. Since the triangle inequalities  $\ell_A - 1 \leq \lambda \leq \ell_A + 1$  and  $\ell_D - 1 \leq \lambda \leq \ell_D + 1$  must be satisfied, only modes satisfying  $\ell_D = \ell_A, \ell_A \pm 2$  have non-zero magnetic coupling. Evaluating the terms appearing in equations (15a) and (15c) for  $\ell_A = m_A$ , the individual terms for the allowed values of  $\lambda$  are

$$\delta B_{A,0}^{\ell_A, \mu} = (-1)^{\ell_A + 1} \sqrt{\frac{(2\ell_A + 1)}{4}} (\ell_A + 1) \sum_{\bar{m}=-1}^{+1} d_{\bar{m}0}^1 \begin{pmatrix} \ell_A & \ell_A & 1 \\ -(\ell_A + \bar{m}) & \ell_A & \bar{m} \end{pmatrix}, \quad (18a)$$

$$\delta B_{A,+}^{\ell_A,\mu} = (-1)^{\ell_A+1} \sqrt{\frac{(2\ell_A+1)(\ell_A+1)}{8\ell_A}} \sum_{\bar{m}=-1}^{+1} d_{\bar{m}0}^1 \begin{pmatrix} \ell_A & \ell_A & 1 \\ -(\ell_A+\bar{m}) & \ell_A & \bar{m} \end{pmatrix}, \quad (18b)$$

$$\delta B_{A,+}^{\ell_A+1,\mu} = (-1)^{\ell_A+1} \sqrt{\frac{(\ell_A+1)(\ell_A+2)}{8\ell_A}} \ell_A^2 \sum_{\bar{m}=-1}^{+1} d_{\bar{m}0}^1 \begin{pmatrix} \ell_A+1 & \ell_A & 1 \\ -(\ell_A+\bar{m}) & \ell_A & \bar{m} \end{pmatrix}, \quad (18c)$$

$$\delta B_{A,+}^{\ell_A-1,\mu} = (-1)^{\ell_A+1} \sqrt{\frac{(\ell_A-1)(\ell_A+1)}{8\ell_A}} (\ell_A+1)^2 \sum_{\bar{m}=-1}^{+1} d_{\bar{m}0}^1 \begin{pmatrix} \ell_A-1 & \ell_A & 1 \\ -(\ell_A+\bar{m}) & \ell_A & \bar{m} \end{pmatrix} \quad (18d)$$

The magnetic coupling coefficients between different r-modes can now be computed. A straight-forward calculation yields the self-coupling term,  $\kappa_{AA}$  as

$$\kappa_{AA} = -\frac{\ell_A+1}{4(2\ell_A+3)} \left\{ \ell_A(\ell_A+1)(\ell_A+2) + 3 + \frac{1}{2} [\ell_A(\ell_A+1)(2\ell_A^2+2\ell_A-3) - 9] \sin^2 \beta \right\}. \quad (19)$$

The off-diagonal term,  $\kappa_{A,A+2}$  and  $\kappa_{A,A-2}$  will be

$$\kappa_{A,A+2} = \kappa_{A+2,A} = -\frac{1}{8} \sqrt{\frac{\ell_A(\ell_A+3)}{(2\ell_A+3)(2\ell_A+5)}} \ell_A(\ell_A+1)(\ell_A+3)^2 \sin^2 \beta, \quad (20a)$$

$$\kappa_{A,A-2} = \kappa_{A-2,A} = -\frac{1}{8} \sqrt{\frac{(\ell_A-2)(\ell_A+1)}{(2\ell_A-1)(2\ell_A+1)}} (\ell_A-2)(\ell_A-1)(\ell_A+1)^2 \sin^2 \beta, \quad (20b)$$

Therefore, the equation of motion for mode's expansion coefficients of the magnetically modified Ath r-modes reduces to

$$\sigma_A c_A = \omega_A \left[ \frac{\mathcal{M}}{2T} |\kappa_{A,A-2}| c_{A-2} + \left( 1 + \frac{\mathcal{M}}{2T} |\kappa_{AA}| \right) c_A + \frac{\mathcal{M}}{2T} |\kappa_{A,A+2}| c_{A+2} \right]. \quad (21)$$

The final equations (19)-(21) give the magnetically corrected eigenfrequencies  $\sigma_A$  and eigenvectors  $c_A$  for the r-modes. To compute these eigenfrequencies and eigenvectors one should solve the  $N$  dimensional linear algebraic system (21), where  $N$  is the number of the modes. Therefore, for a given  $N = 1, 2, \dots$ , the  $N \times N$  matrix should be diagonalized. Since it is not possible to solve an infinite dimensions system in practice, we truncate the infinite matrix to a finite matrix and large enough  $N$ . Further we note that for the lower inclination angles, the magnetic coupling coefficients  $|\kappa_{AD}|$  increase by  $\ell_A^3$ , while for the larger inclination angles by  $\ell_A^4$ . Since we are working in the linear regime, we have to keep  $(\mathcal{M}/2T) |\kappa_{AA}| < 1$ . The ratio of magnetic energy density to rotational energy density in the covered ocean at the surface of star is

$$\frac{\mathcal{M}}{2T} = 8 \times 10^{-3} \left( \frac{B}{10^{14} \text{ G}} \right)^2 \left( \frac{10^9 \text{ g cm}^{-3}}{\rho} \right) \left( \frac{10 \text{ km}}{R} \right)^2 \left( \frac{10^3 \text{ Hz}}{\Omega} \right)^2, \quad (22)$$

where  $\rho$  is the ocean's density. In tables 1 and 2 we present the eigenfrequencies of  $\ell_A = m_A = 1, 2, \dots, 6$  r-modes. In table 1 we assume the inclination angle between field axis and shell's spin axis is zero,  $\beta = 0$ , and calculate the eigenfrequencies  $\sigma_A$  for different ratio of the magnetic energy density to the rotational energy density,  $\mathcal{M}/2\mathcal{T}$ , by increasing the magnetic field strength, see equation (22). In table 2 we compute the eigenfrequencies by increasing the inclination angle for a specific energy ratio  $\mathcal{M}/2\mathcal{T} = 10^{-2}$ . As a result, the eigenfrequency of the mode increases by increasing both magnetic field energy density and inclination angle.

In the next section we consider the kinematical secular effects of r-modes in the oceanic fluid.

### 3. The r-mode drift by the magnetic field

In a series of papers Rezzolla et al. (2000, 2001a,b) showed the existence of kinematical secular velocity field of r-mode oscillations which interacts with the background magnetic field of the star. Although, this interaction is non-linear and should be considered in non-linear regime, one can find some second-order quantities from linear result (Rezzolla et al. 2000). As an example, the second-order secular toroidal drift which appear on isobaric surfaces, can be obtained through the linear velocity field.

To investigate this secular effect in the fluid motion undergoing the magnetic corrected r-mode oscillations in the ocean fluid, we consider the real part of the magnetic corrected fluid velocity of  $\ell_A = m_A$  r-mode, equation (2),

$$\dot{\theta}(t) = - \sum_A \alpha Q(\ell_A) c_A \hat{\sigma}_A (\sin \theta)^{\ell_A-1} \cos(\ell_A \phi - 2\pi \hat{\sigma}_A t), \quad (23a)$$

$$\dot{\phi}(t) = \sum_A \alpha Q(\ell_A) c_A \hat{\sigma}_A \cos \theta (\sin \theta)^{\ell_A-2} \sin(\ell_A \phi - 2\pi \hat{\sigma}_A t), \quad (23b)$$

where  $\hat{\sigma}_A = \sigma_A/\Omega$  and

$$Q(\ell_A) = \left(-\frac{1}{2}\right)^{\ell_A} \frac{1}{\ell_A!} \sqrt{\pi \ell_A (\ell_A + 1) (2\ell_A + 1)!/4}. \quad (23c)$$

In equations (23)  $\sigma_A$  and  $c_A$  are the magnetic corrected eigenfrequency and eigenvector, respectively, and the time,  $t$ , is in unit of the star's period,  $P$ .



In figures 1 to 3 we plotted the result of numerical integration of equations (23) in the shell’s northern hemisphere for the magnetic corrected  $\ell_A = m_A = 2$  r-mode with amplitude  $\alpha = 0.1$ . Note, we assumed that at  $t = 0$  the only  $\ell_A = m_A = 2$  r-mode is present in the fluid and all calculations are done in the corotating frame.

In the case of zero inclination angle,  $\beta = 0$ , our results for all mode’s latitudes are in good agreement to those results which have been reported by Rezzolla et al. (2000, 2001a). In figure 1 we plotted  $\theta(t)$  vs  $\phi(t)$  from  $t = 0$  to  $t = 7.45P$  (almost 5 cycles of the mode), with initial values  $\phi(0) = 0$ ,  $\theta(0) = \pi/2$ ,  $\ell_A = m_A = 2$ , zero inclination angle  $\beta = 0$ , and two different values of  $\mathcal{M}/2\mathcal{T} = 0$  and  $10^{-1}$ . The aligned field causes the drift in  $\phi$ -direction (produced by the r-mode) to increase. The corrected expression for the drift velocity of a given fluid element in the background of the uniform magnetic field will be <sup>2</sup>

$$\mathbf{v}_d = \sum_A K_A(\theta) \alpha(t) \sigma_A(t) \mathbf{e}_\phi, \quad (24)$$

$$K_A(\theta) = Q^2(\ell_A) c_A^2 (\sin \theta)^{2\ell_A-4} \left[ \sin^2 \theta - 2(\ell_A - 1) \cos^2 \theta \right]. \quad (24a)$$

As a result, because of nonzero inclination angle, the drift velocity of a fluid element undergoing the  $\ell_A$  r-mode oscillation is affected by all  $\ell_A \pm 2$  r-mode oscillations. Equation (24) reduces to one obtained by Rezzolla et al. (2000, 2001a), for the non-magnetic  $\ell_A = m_A = 2$  r-mode, ie.  $\mathbf{v}_d = K_2(\theta) \alpha(t) \omega_2(t) \mathbf{e}_\phi$ . Therefore, the total displacement in  $\phi$  from the onset of the oscillation at  $t_0$  to time  $t$  is

$$\Delta\phi(\theta, t) = \sum_A K_A(\theta) \int_{t_0}^t \alpha^2(t') \sigma_A(t') dt'. \quad (25)$$

The change in  $\phi$  due to the magnetic field is given in tables 3 and 4. As a result,  $\Delta\phi = \phi_{\text{mag}} - \phi_{\text{nonmag}}$  increases by increasing the magnetic energy density. Further the high- $\ell_A$  magnetic r-modes are drifted more than the low- $\ell_A$  ones.

As shown in figures 2 and 3, the r-mode trajectories in both  $\theta$ - and  $\phi$ -directions are strongly modulated by the inclined magnetic field. In figure 2 from left to right, we plotted time evolution of r-mode displacements in  $\theta$ -direction, in  $\phi$ -direction, and the projected  $(\theta, \phi)$  r-mode trajectory, respectively. All panels correspond to  $\mathcal{M}/2\mathcal{T} = 10^{-2}$  and are plotted with initial conditions  $\phi(0) = 0$ ,  $\theta(0) = \pi/2$ . The inclination angle is  $\beta = 0$  for

---

<sup>2</sup>Following Rezzolla et al. (2000, 2001a) equation (24) is obtained by expanding equations (23) in powers of  $\alpha$ , averaging over a gyration, and retaining only the lowest-order nonvanishing term.

the top,  $\beta = \pi/6$  for the middle, and  $\beta = \pi/2$  for the bottom panels. The larger the field's angle the stronger the modulation. First and second columns of figure 2 show how  $\theta$ - and  $\phi$ - displacements of the initial  $\ell_A = m_A = 2$  r-mode are affected by the inclined field, respectively. In the third column we show the motion of fluid element in the northern hemisphere of the shell undergoing the  $\ell_A = m_A = 2$  r-mode oscillations. The projected trajectories  $\theta(t) \sin \theta(t) \cos \phi(t)$  and  $\phi(t) \sin \theta(t) \cos \phi(t)$  show how the inclined magnetic field change the motions which will be detected by a distance corotating observer in the rotation equator of the shell. It is interesting to note that the results show the coupling coefficients are more sensitive to the field inclination angle rather than the magnetic field strength.

Furthermore, the larger the fluid element's latitude, the stronger the modulation. This feature is shown in figure 3 which is plotted by different initial conditions  $\phi(0) = 0$ ,  $\theta(0) = \pi/6$  for both  $\beta = 0$  (the top panels) and  $\beta = \pi/2$  (the bottom panels). Comparing both bottom panels in figures 2 and 3 reveals that the magnetic field (having the same energy density and inclination angle) has less effect on the lower latitude modes.

Finally we note that  $\Delta\phi$  also increases by increasing the inclination angle, see the third column of figures 2 and 3. Therefore, the motion of a fluid element of the shell undergoing the magnetic r-mode oscillation is drifted more than nonmagnetic r-mode oscillation both by field energy density and field inclination angle. These properties can be understood by considering both  $\Delta\phi$  and  $\mathbf{v}_d$  are proportional to the corrected eigenfrequency and eigenvector, see equations (24) and (25). The corrected eigenvector changes by changing inclination angle while the corrected eigenfrequency increases by increasing field energy density.

The toroidal fluid motions produced by r-mode are perpendicular to the magnetic field. They distort the field and increase the field energy density. As shown by Rezzolla et al. (2000) if the energy that it needs to distort the magnetic field required by the mode is greater than the mode energy during an r-mode oscillation, the distortion of the magnetic field which is proportional to the  $\mathbf{v}_d$ , will prevent the oscillation from occurring. To make an estimate at which field strength the distortion effect might get to be important we calculate the ratio of the change in the magnetic energy density of the shell,  $\delta E_m = \int (\delta B^2 / 4\pi) d\Omega$ , to the mode energy density during one oscillation as

$$\frac{\delta E_m}{\epsilon_A} \approx \frac{\mathcal{M}}{2T} |\kappa_{AA}|, \quad (26)$$

$$\approx 10 \left( \frac{B}{10^{16} \text{ G}} \right)^2 \left( \frac{10^9 \text{ g cm}^{-3}}{\rho} \right) \left( \frac{10 \text{ km}}{R} \right)^2 \left( \frac{10^3 \text{ Hz}}{\Omega} \right)^2 \begin{cases} \ell_A^3 & \text{for small } \beta \\ \ell_A^4 & \text{for large } \beta \end{cases} \quad (26a)$$

Thus  $\delta E_m > \epsilon_A$  if  $B > B_{\text{critical}} \approx 3 \times 10^{15} \rho_9 R_{10} \Omega_3 \ell_A^\eta$ , where  $\eta = -3/2$  and  $\eta = -2$  for small and large inclination angles, respectively. Here  $\rho_9 = \rho/10^9 \text{ g cm}^{-3}$ ,  $R_{10} = R/10 \text{ km}$ , and  $\Omega_3 = \Omega/10^3 \text{ s}^{-1}$ . Hence the smaller field strength would prevent the high- $\ell_A$  r-mode oscillations. Further, equation (26) shows that for the higher field inclination angle the distortion effect will be stronger.

In addition the increase in the energy of the magnetic field produced by the r-mode drift reduces the mode energy and causes damping. The rate that the magnetic field extracts energy density from the mode can be estimated by

$$(1/4\pi) \int B_\phi (dB_\phi/dt) d\Omega \approx \sum_A K_A(\theta) \alpha^2 \sigma_A B_p B_\phi. \quad (27)$$

The azimuthal field  $B_\phi$  is generated by r-mode drift velocity  $\mathbf{v}_d$  from the background poloidal field. The change in  $B_\phi$  can be calculated approximately for the magnetic r-modes from the time  $t_0$  that the oscillation begins to time  $t$  by  $\Delta B_\phi(t) \approx \sum_A \int_{t_0}^t K_A(\theta) \alpha^2(t) \sigma_A(t) B_p dt$  (Rezzolla et al. 2000). Equation (27) shows that the losing energy of the mode increases by increasing the field energy density and the inclination angle. Furthermore, since the high- $\ell_A$  magnetic r-modes are drifted more than the low- $\ell_A$  ones, they will damp faster than the low- $\ell_A$  modes.

## 4. Discussion

In this paper, by assuming neutron stars in the low-mass X-ray binaries (LMXBs) are covered by degenerate massive oceans, we have studied the interaction of the inclined magnetic field with r-mode oscillations of an incompressible ocean fluid in a thin shell approximation. Our analysis shows that even for weak magnetic field energy density in comparison with the star's rotational energy density,  $\ell$  and  $\ell \pm 2$  r-modes are coupled significantly.

The kinematical secular drift produced by the r-mode, is studied in the background of the inclined magnetic field. The results show that the magnetic field tends to increase the fluid drift in the  $\phi$ -direction. As a result, for the same time period, the fluids in the presence of the magnetic field undergo larger drift than fluids with no background magnetic field.

Since the magnetic field is distorted by the r-mode, we showed that the field distortion by the high- $\ell$  magnetic r-mode is stronger than the low- $\ell$  modes. Thus a smaller critical field is needed to prevent the high- $\ell$  r-mode oscillation from occurring. Further, the shear

produced by the drift velocity of the magnetic r-mode will damp high- $\ell$  modes faster than the low- $\ell$  ones. Note that in the present paper, we assume the r-mode is stable, so we do not deal with its unstable growth in the magnetic star as has been considered by Rezzolla et al. (2000).

Observational and phenomenological studies of more than twenty LMXBs reveal that these accreting neutron stars are source of millisecond oscillations, burst oscillations, and quasi-periodic oscillations in Hz-kHz range. Different authors proposed different possible mechanisms to explain the observations in LMXBs, but the regularity of these oscillations in many sources led the investigators to consider radial or nonradial oscillations in a coronal accretion flow near the Eddington limit, see the review by van der Klis (2000). By assuming neutron stars in LMXBs covered by an ocean fluid Bildsten et al. (1995, 1996) showed that both low and high radial orders of ocean g-modes might be responsible for observed low frequency ( $\sim$  Hz) oscillations in these stars. Recently Heyl (2001) discussed different possible oscillations (the g-modes, the Kelvin modes, and the buoyant r-modes) that may excite in the neutron star ocean during a Type-I burst, and concluded that the buoyant r-modes may meet the observations of low frequency oscillations in Type-I X-ray bursts quite well.

Figures 2 and 3 show how the inclined magnetic field modulates  $\ell_A = m_A = 2$  r-modes. The associated envelope frequency,  $f_{\text{envelope}}$ , decreases as  $f_{\text{envelope}} \sim \nu_s/10 - \nu_s/16$  when the inclination angle increases from  $\beta \sim \pi/6 - \pi/2$ . Here  $\nu_s = \Omega/2\pi$  is the star’s spin frequency. The frequencies of these new modes are comparable to those observed oscillations in the LMXBs in low frequencies. For the star’s spin frequency  $\nu_s \approx 300$  Hz, the wave envelope frequency is  $f_{\text{envelope}} \sim 20 - 30$  Hz. Different frequencies may be obtained by different initial  $\ell_A = m_A$  r-modes. Further, the amplitude of the modulated oscillations increases by increasing the inclination angle and/or mode’s altitude.

Though there is still no firm observational evidence for the low magnetic field strength in the LMXBs, these objects are believed to be neutron stars with weak magnetic fields ( $B \lesssim 10^9$  G), high accretion rates ( $\dot{M} \gtrsim 10^{-9} M_\odot \text{ yr}^{-1}$ ), and milliseconds spin frequencies (van der Klis 2000). Our calculations show the existence of an inclined (even weak) magnetic field modulates the normal modes of an ocean fluid to a new mode with frequency  $f_{\text{envelope}}$ . Therefore, by observing normal modes in the neutron star’s ocean, one would be expecting to observe these new modes.

The author is grateful to S. M. Morsink and S. Sengupta for reading the manuscript and

numerous discussions. This research was supported by the Natural Sciences and Engineering Research Council of Canada.

## REFERENCES

- Bildsten, L. 1993, ApJ, 418, L21
- Bildsten, L. 1995, ApJ, 438, 852
- Bildsten, L., & Cutler, C. 1995, ApJ, 449, 800
- Bildsten, L., Ushomirsky, G., & Cutler, C. 1995, ApJ, 449, 800
- Campbell, W. B. 1971, J. Math. Phys., 12, 1763
- Edmonds, A. R. 1974, *Angular Momentum in Quantum Mechanics*, second edition with corrections, (Princeton, NJ: Princeton University Press)
- Fushiki, I. & Lamb, D. Q. 1987, ApJ, 323, L55
- Heyl, J. 2001, preprint, astro-ph/0108450
- Hide, R. 1966, Phil. Trans. Royal Soc. London, Series A, 259, 615
- Jackson, J. D. 1975, *Classical Electrodynamics*, 2nd Edition, (New York, NY, John Wiley & Sons)
- Lenin, Y., Ushomirsky, G. 2001, MNRAS, 322, 515L
- Morsink, S. M., & Rezanian, V. 2002, submitted to ApJ
- Rezzolla, L., Lamb, F. K., & Shapiro, S. L. 2000, ApJ, 531, L141
- Rezzolla, L., Lamb, F. K., Marković, D., & Shapiro, S. L. 2001a, Phys. Rev. D, to appear, gr-qc/0107061
- Rezzolla, L., Lamb, F. K., Marković, D., & Shapiro, S. L. 2001b, Phys. Rev. D, to appear, gr-qc/0107062
- Schenk, A. K., Arras, P., Flanagan, É. É., Teukolsky, S. A., & Wasserman, I., 2001, Phys. Rev. D, to appear, gr-qc/0101092

Stewartson, K. 1967, Proc. Royal Soc. London, Series A, 299, 173

van der Klis, M. 1995, in X-ray Binaries, ed. W. H. G. Lewin, J. van Paradjis, & E. P. J. van den Heuvel (Cambridge: Cambridge University Press), 252

van der Klis, M. 2000, Annual Review of Astronomy and Astrophysics, 38, 717

Table 1. The eigenfrequency of  $\ell_A = m_A$  r-modes in the thin shell in the presence of a uniform magnetic field,  $\sigma_A/\Omega$ . The angle between magnetic field axis and shell’s spin axis is  $\beta = 0$ . The energy in the magnetic field is  $\mathcal{M} = B_p^2/4\pi$  and the rotational energy is  $\mathcal{T} = \rho a^2 \Omega^2/2$ . A number  $a \times 10^{\pm b}$  is written as  $a \pm b$ .

$\mathcal{M}/2\mathcal{T}$	$\ell_A = 1$	$\ell_A = 2$	$\ell_A = 3$	$\ell_A = 4$	$\ell_A = 5$	$\ell_A = 6$
0.0	-.10000+01	-.66667+00	-.50000+00	-.40000+00	-.33333+00	-.28571+00
1.0-04	-.10000+01	-.66686+00	-.50004+00	-.40056+00	-.33415+00	-.28684+00
1.0-03	-.10005+01	-.66943+00	-.50838+00	-.41797+00	-.37886+00	-
1.0-02	-.10090+01	-.68595+00	-.53500+00	-.45591+00	-	-

Table 2. The eigenfrequency of  $\ell_A = m_A$  r-modes in the thin shell in the presence of a uniform magnetic field,  $\sigma_A/\Omega$  for different value of inclination angle,  $\beta$ . The ratio of magnetic energy to the rotational energy is  $\mathcal{M}/2\mathcal{T} = 10^{-2}$ . A number  $a \times 10^{\pm b}$  is written as  $a \pm b$ .

$\beta$	$\ell_A = 1$	$\ell_A = 2$	$\ell_A = 3$
0.0	-.10090+01	-.68595+00	-.53500+00
$\pi/6$	-.10080+01	-.68874+00	-.54775+00
$\pi/4$	-.10068+01	-.69038+00	-.55827+00
$\pi/3$	-.10056+01	-.69155+00	-.56837+00
$\pi/2$	-.10043+01	-.69250+00	-.57834+00



Table 3. Change in displacement  $\phi$ ,  $\Delta\phi = \phi_{mag} - \phi_{nonmag}$  for  $\ell_A = m_A = 2$  r-mode, due to the magnetic field, from  $t = 0$  to  $t = 7.45P$ . Initial values  $\phi(0) = 0$ ,  $\theta(0) = \pi/2$  and zero inclination angle  $\beta = 0$  are considered. A number  $a \times 10^{\pm b}$  is written as  $a \pm b$ .

$\mathcal{M}/2\mathcal{T}$	$\Delta\phi$
0.0	0.0
1.0-04	.36403-06
1.0-03	.19299-05
1.0-02	.29707-03
1.0-01	.10390-01

Table 4. Change in displacement  $\phi$ ,  
 $\Delta\phi = \phi_{mag} - \phi_{nonmag}$  for different  $\ell_A = m_A$  r-mode,  
due to the magnetic field, from  $t = 0$  to  $t = 7.45P$ .  
Initial values  $\phi(0) = 0$ ,  $\theta(0) = \pi/2$ ,  $\mathcal{M}/2\mathcal{T} = 10^{-2}$  and  
zero inclination angle  $\beta = 0$  are considered. A number  
 $a \times 10^{\pm b}$  is written as  $a \pm b$ .

$\ell_A = m_A$	$\Delta\phi$
1	.56340-06
2	.29707-04
3	.39012-03
4	.14556-02

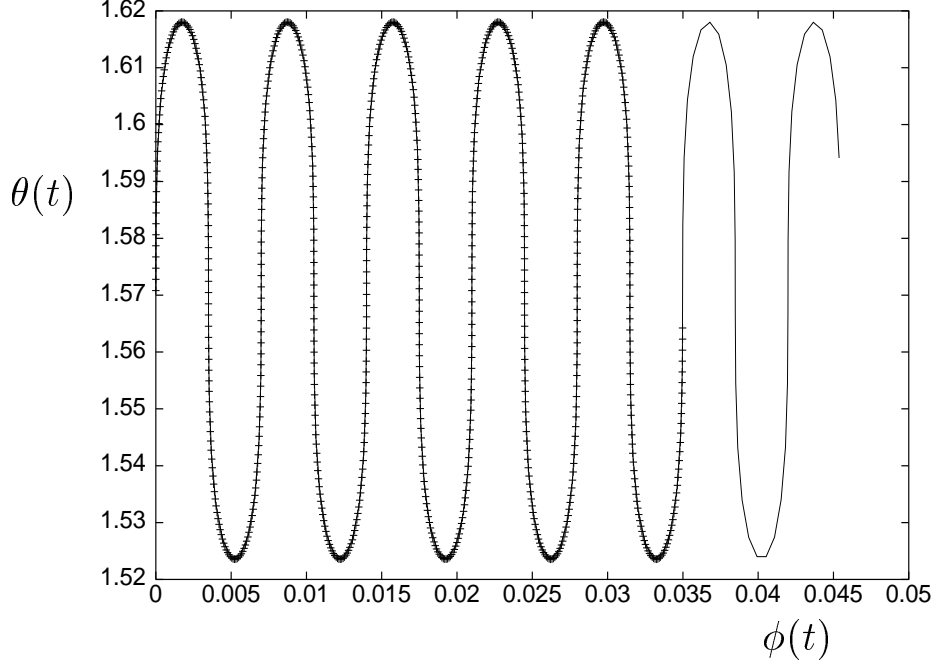


Fig. 1.— Motion of a fiducial fluid element in the northern hemisphere of a shell undergoing  $\ell_A = m_A = 2$  r-mode with amplitude  $\alpha = 0.1$ . The projected trajectories are plotted for 7.45 of period of star (almost 5 cycles of the mode), with initial values  $\phi(0) = 0$ ,  $\theta(0) = \pi/2$  and zero inclination angle  $\beta = 0$ . The dash sign refers to zero magnetic field,  $\mathcal{M} = 0$ , while the continuous line corresponds to assumed value  $\mathcal{M}/2\mathcal{T} = 10^{-1}$ . Both  $\theta$  and  $\phi$  are in radian.

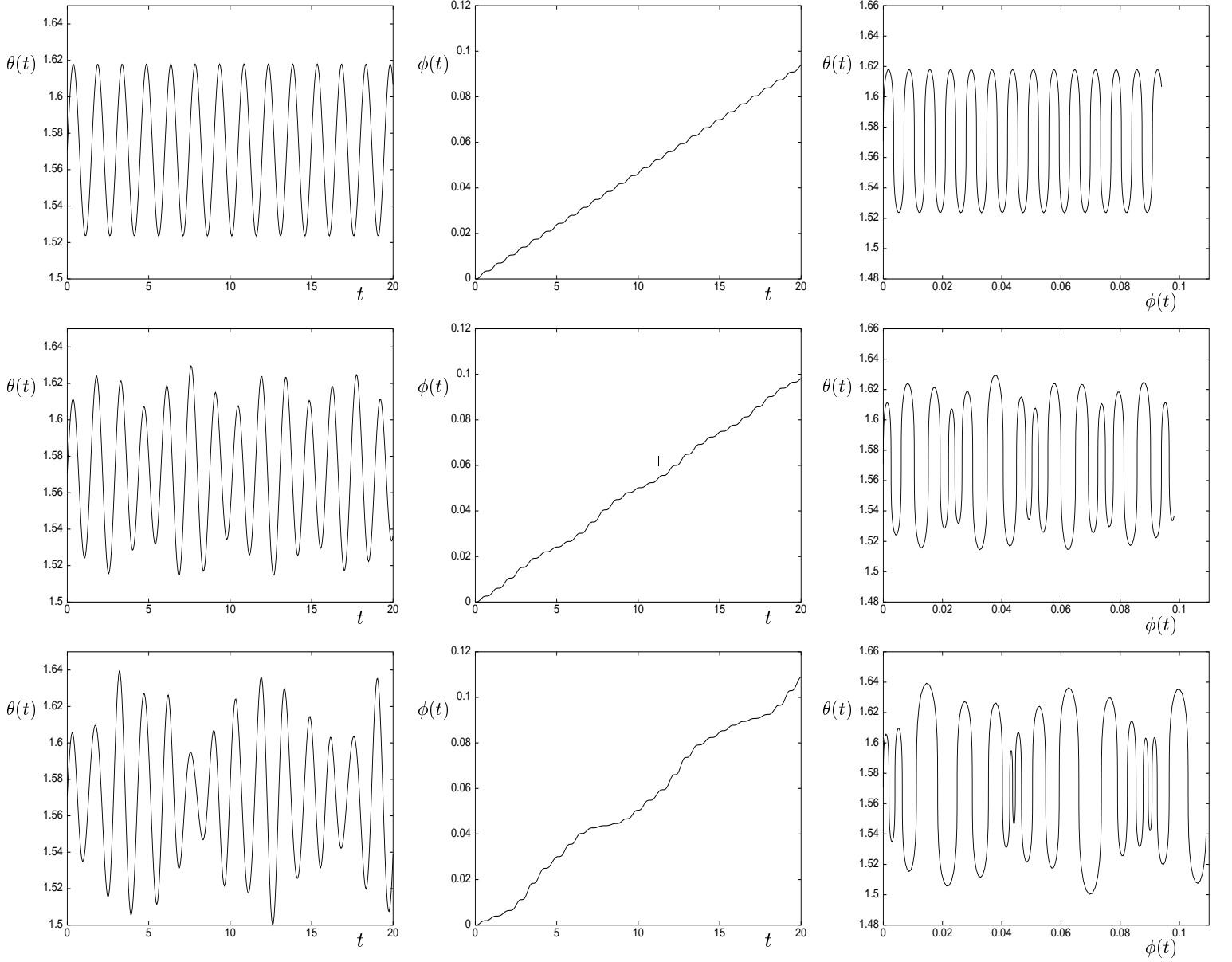


Fig. 2.— Motion of a fiducial fluid element in the northern hemisphere of a shell undergoing  $\ell_A = m_A = 2$  r-mode with amplitude  $\alpha = 0.1$ . The projected trajectories are plotted for 20 of period of star (almost 13 cycles of the mode), with initial values  $\phi(0) = 0$ ,  $\theta(0) = \pi/2$  and  $\mathcal{M}/2\mathcal{T} = 10^{-2}$ . Both  $\theta$  and  $\phi$  are in radian and  $t$  is in unit of star's period,  $P$ . (a) The top panels are plotted for  $\beta = 0$ , (b) The middle panels are plotted for  $\beta = \pi/6$ , (c) The bottom panels are plotted for  $\beta = \pi/2$ .

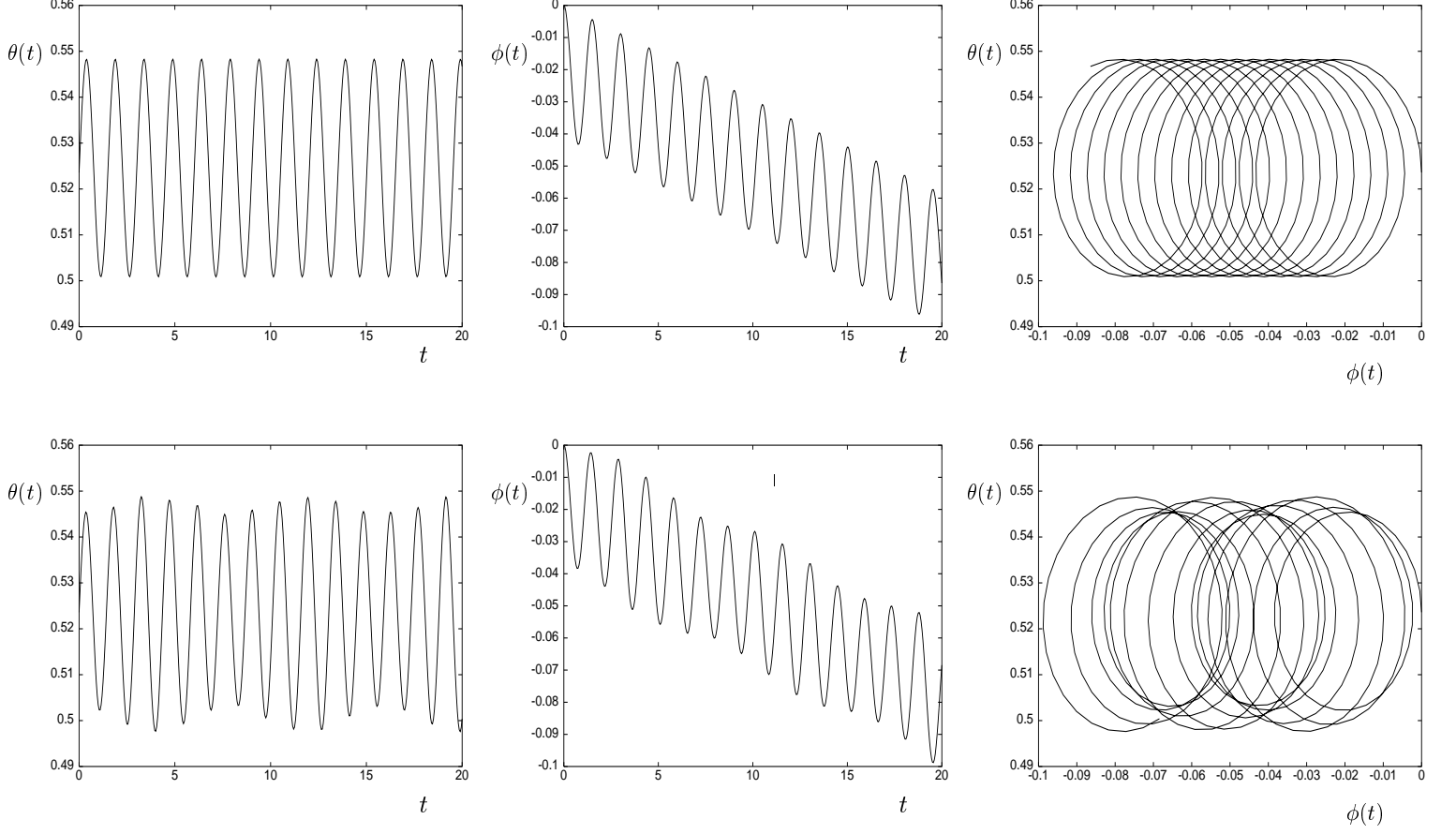


Fig. 3.— Same as figure 2 with initial values  $\phi(0) = 0$ ,  $\theta(0) = \pi/6$ . (a) The top panels are plotted for  $\beta = 0$ , (b) The bottom panels are plotted for  $\beta = \pi/2$ .